Jurnal Teknologi

Full Paper

EFFECT OF SN COMPONENT ON PROPERTIES AND MICROSTRUCTURE CU-NI-SN ALLOYS

D. N. Nguyen[a*], A. T. Hoang[b], X. D. Pham[a], M. T. Sai[c], M. Q. Chau[d], V. V. Pham[a]

[a]School of Mechanical Engineering, Vietnam Maritime University, Lach Tray Road, Haiphong, Vietnam
[b]Faculty of Mechanical Engineering, Ho Chi Minh city University of Transport, D3 Road, Ho Chi Minh City, Vietnam
[c]Faculty of Mechanical Engineering, Le Quy Don University, Hoang Quoc Viet Road, Hanoi, Vietnam.
[d]Faculty of Mechanical Engineering, Industrial University of Ho Chi Minh, Nguyen Van Bao Road, Ho Chi Minh City, Vietnam

Article history
Received
29 October 2017
Received in revised form
4 June 2018
Accepted
15 June 2018
Published online
5 October 2018

*Corresponding author
namnd.khcs@vimaru.edu.vn

Graphical abstract

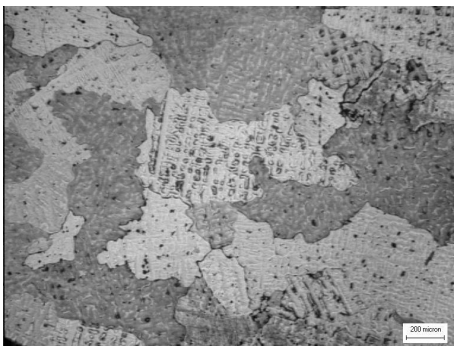

Abstract

This paper investigates a high electrical conductivity and high strength of alloys based on Cu-Ni-Si system It proclaimed the results of the effect of tin (Sn) component on the mechanical properties and microstructure of Cu-Ni-Sn alloy. The conditions for processing the Cu-Ni-Si alloy were presented, the analysis of microstructure and mechanical properties after heat treatment was examined by X-ray, SEM, EDS and specialized machines. The results showed that with 3% mass of Sn added into the Cu-Ni-Sn alloy along with heat treatment and deformation, the hardness value reached the range of 221-240HV, the tensile strength and elastic limit reached around 1060MPa and 903MPa respectively. However, after heat treatment and deformation for the Cu-Ni-Sn alloy based on 6% mass of Sn, the hardness value reached the range of 221-318HV, the tensile strength and elastic limit were respectively 222MPa and 263MPa higher than those of the Cu-Ni-Sn alloy with 3% mass of Sn. The result from X-ray analysis showed the deflection of peaks. Nonetheless, the new phases were not observed in SEM and EDS, contrariwise, generated modular structure was considered as the proof of the Spinodal cluster. This fact might be explained by two mechanisms: deformation mechanism and Spinodal decomposition.

Keywords: Spinodal decomposition, deformation mechanism, Cu-Ni-Sn alloy, mechanical property, microstructure

1.0 INTRODUCTION

The strength and hardness of materials are extremely important mechanical properties. The enhancement of the materials can be done by using different techniques like the refinement of the particle size, hardened-strain, hardened - solid solution, hardened-quench, strengthened-dispersion, and hardened-precipitation [1]. The heating method also considered as a simple technique [2]. The hardening process by Spinodal decomposition applied to copper alloys is an emerging technique for the strengthening of copper [3]. The Spinodal decomposition alludes to a process when the supersaturated solid-solution may decompose into the regions such as solute-rich/solute-depleted ones after being aged at an appropriate

temperature [4]. The strain regions around the Spinodal decomposition with the arranged structure interrupt the motion of the dislocation, thus, the increase in the hardness occurs [5]. The increase in the alloy strength, even by three times during the aging process, depends on the alloy composition, the colling level before aging, and the aging temperature [6].

Spinodal decomposition is fine, homogeneous two-phase mixtures, which produced in original phases, separated under certain conditions of the temperature and composition such as in a supersaturated solid solution of metals including the same size of atoms [7]. In Spinodal decomposition, the original phases spontaneously decompose into other phases where the crystal structure stays the same, but the atoms in the crystals are different [8]. Although the size of the atoms is the same, the treated Spinodal structure based on the heat retains the same geometry as the original, and the structure does not distort during heat treatment. Spinodal decomposition is possibly happens when the metal atoms in the alloy are nearly similar in size size and can form a completely homogeneous solid solution [9]. Using thermodynamic principles, Vander Waals was able to explain the presence of a "horizontal cusp" in entropy-versus-volume curves for fluids, and he identified Spinodal in other systems as well. J. Willard Gibbs used the model of free energy and composition diagrams to rationalize the limits of phase metastability in ceramics and alloys, and he described the transformation as Spinodal decomposition [10].

Based on the study and the application of Spinodal decomposition for coppery alloys, ternary copper-nickel-tin Spinodal alloys have been recently developed to deliver larger sizes and engineered shapes with a combination of high strength, high electrical conductivity excellent tribological characteristics, and high corrosion resistance in seawater and acid environments [10]. The U.S.Pat.No. 4373970 [12] disclosed Spinodal alloys, containing from five to thirty-five weight percent of nickel, from about seven to thirteen weight percent of tin, and the balance copper.

Several studies were carried out with the alloys of Spinodal bronze (Cu-Ni-Sn) in order to determine the mechanical properties and the microstructures [13, 14]. Besides, other studies were also carried out to evaluate the wear behavior while these alloys were used in case of high performance and wearability. The study result of wear behavior and microstructure involved to the hardness of Cu-Ni-Sn spinodal alloy are presented by Zhang *et al.* [15, 16]. The influence of Sn component on the Cu-Ni-Sn alloy hardness while 10% of Ni weight was kept fixedly when the experiment was conducted [17]. Furthermore, cooling in both rapid and normal methods to evaluate the effect of temperature on Cu-Ni-Sn alloys mechanical properties and microstructure was used and presented by Marcella *et al*. [18]. Moreover, the study on producing the alloys with high strength and high electrical conductivity based on the Cu-Ni-Sn system were shown worth-surprising results [19, 20]. A large of precipitated nanoscale quantity might be formed during aging, and the result shows increasing in strength but sacrificing insignificantly of electrical conductivity in Cu-Ni-Sn alloys [21].

Until now, Spinodal copper alloys have been commercially available only in thin sections and limited temper options. Most copper-based alloys showed high strength from solid-solution hardening, cold working, precipitation hardening, or by a combination of these strengthening mechanisms [22]. However, in the ternary copper-nickel-tin alloys, high mechanical strength is produced by a controlled heat treatment that is called Spinodal decomposition.

In this study, the effects of Sn composition on the microstructure of Cu-Ni-Sn alloys were analyzed by X-ray, SEM, and EDS. Furthermore, mechanical properties and electrical conductivity of Cu-Ni-Sn alloys based on the changes of the mass of Sn were also tested. Besides, the effect of Spinodal decomposition on the microstructure and mechanical properties of Cu-Ni-Sn alloys was also thoroughly explained.

2.0 METHODOLOGY

2.1 Materials

In this study, S_1 and S_2 samples were used when the experiment was conducted. The element components of these samples were given in Table 1.

Table 1 The composition of alloy samples

No	Cu (%wt)	Ni (%wt)	Sn (%wt)	Sample
1	88.50	8.27	2.99	S_1 (Cu-9Ni-3Sn)
2	83.30	9.94	6.43	S_2 (Cu-9Ni-6Sn)

The samples of Cu-9Ni-3Sn; Cu-9Ni-6Sn alloys were quenching at high temperature (850°C) aiming at nickel (Ni) and tin (Sn) being dissolved completely in copper (Cu), a solid solution could keep unstable at room temperature, strain, and tempering. As strain and tempering, unstable solid solution decomposed to richen Sn atom clusters with nanometer-size, and homogeneous distribution increased the strength of alloys. This was an important characteristic for improving the mechanical property of Cu-Ni-Sn alloys, which were similar to the properties of copper-beryllium alloys. For furtherSpinodal decomposition to occur it was necessary to take heat treatment combined with the strain.

2.2 Methods

The samples of Cu-9Ni-3Sn and Cu-9Ni-6Sn alloys were kept at 850°C to produce the solid solution, and quenching in water to produce an unstable solid solution. The samples were tempered at 350°C, and hold in two hours. At this condition, the solid solution

was decomposed. Before and after treatment, the samples were observed the microstructure by using Axiovert 100A microscope, tested the hardness by using 1 kg of the load with Duramin 2 machine. After cold-rolled and tempered at 350°C in 2 hours, the samples are observed the microstructure by using Scanning electron microscopy. The electrical conductivity was measured by RLC LEADER. The strength samples are made on the machine WP 300. Besides, the microstructure of Cu-Ni-Sn is analyzed by X-ray diffraction and FESEM, microscopy, mechanical properties and electrical conductivity are tested in order to prove the effect of tin on the properties and microstructure.

3.0 RESULTS AND DISCUSSION

3.1 Microstructure and Mechanical Properties

The experimental results in Figure 1 show that the microstructure of Cu-9Ni-3Sn alloy has dendrites after casting, the grain size is about 200µm. The average hardness value of the S1's sample is lower than the S2's sample and it is displayed in Table 2.

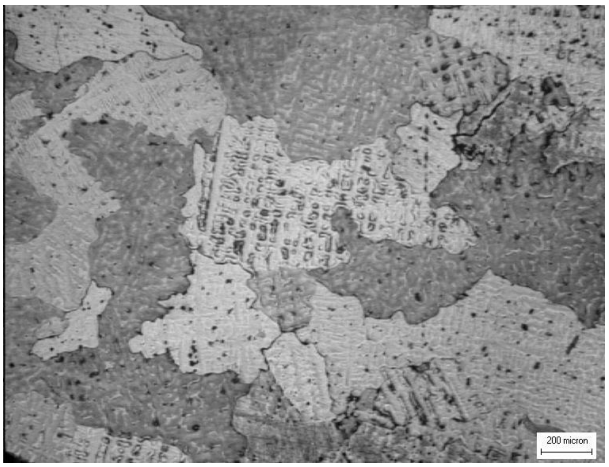

Figure 1 Microstructure of Cu-9Ni-3Sn after casting

Table 2 Vickers hardness (HV of samples after casting

Sample	S_1	S_2
HV	110	125

The average hardness values of the samples are the same. In Figure 2, it is shown that after quenching, the microstructure of Cu-9Ni-6Sn alloy is uniform, and the grain size about 150µm is smaller after casting. The hardness is decreased. This may be due to the uniform and fine microstructure that causes the decrease of the strength. The hardness (HV) of Cu-9Ni-6Sn sample after quenching is given in Table 3.

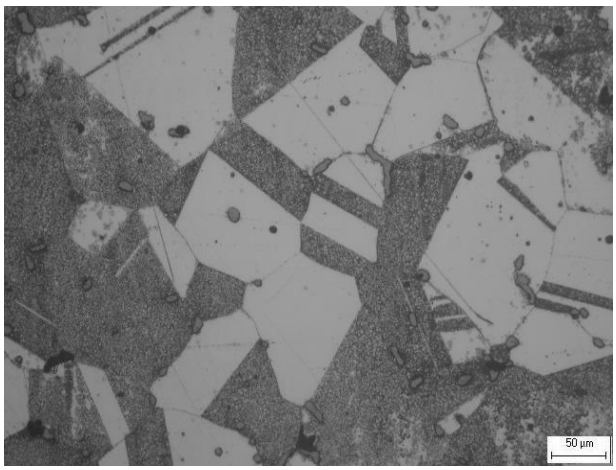

Figure 2 Microstructure of Cu-9Ni-6Sn after quenching

Table 3 Vickers hardness (HV) of samples after quenching

Sample	S_1	S_2
HV	98	105

The mechanical properties changed more when assembling the quenching and tempering within two hours. After tempering, the average hardness of the samples increased. However, the hardness of S_1 has a minimum value, while the hardness of S_2 has a maximum value. This fact may be because of the increase in %Sn of mass. The hardness of the samples (HV) after tempering is shown in Table 4.

Table 4 Vickers hardness (HV) of samples after tempering

Sample	S_1	S_2
HV	151	271

After strain and tempering, the microstructure of Cu-9Ni-3Sn and Cu-9Ni-6Sn alloy is uniform, corresponding to about 60µm of grain size smaller than after quenching. The result can be observed clearly in Figure 3 and Figure 4.

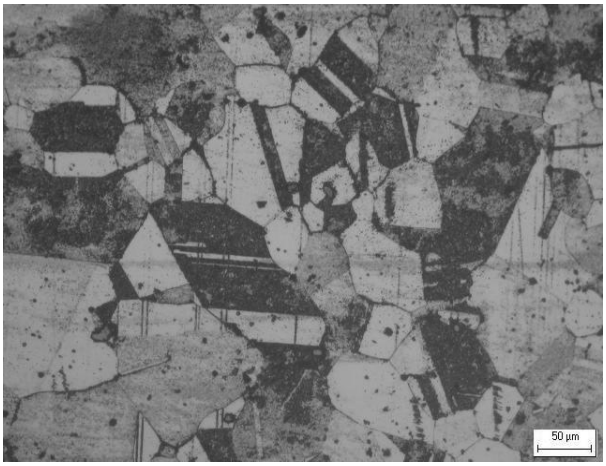

Figure 3 Microstructure of Cu-9Ni-3Sn after strain and tempering

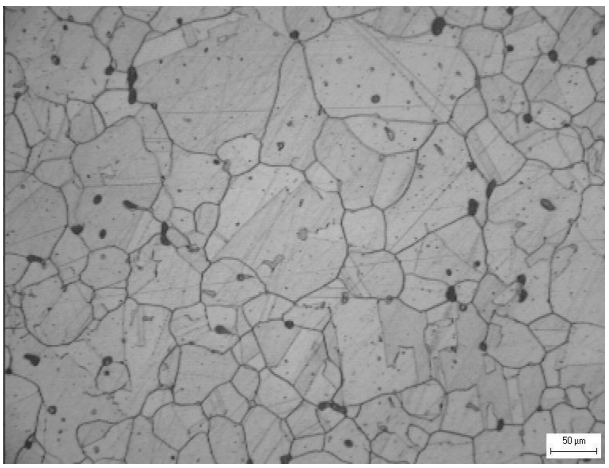

Figure 4 Microstructure of Cu-9Ni-6Sn after strain and tempering

From Figure 3 and Figure 4, it can be seen clearly that the grain size after tempering compared to quenching decreased distinctly (about 70 - 80µm). The grain is more uniform and the reduced size in grain is because of the secretion phase and division resulted from a grain separation. The microstructure of the twinning after quenching may be seen.

The comparison of casting and quenching is shown in Figure 5 and Figure 6, the sample strength increases after quenching, strain, and tempering. This strength value is as same as the yield strength.

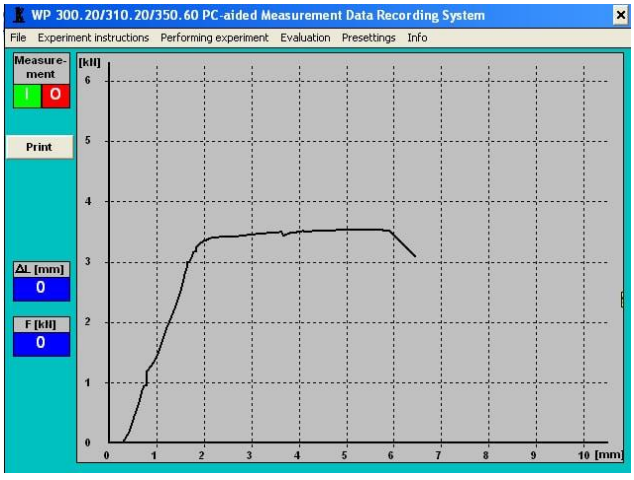

Figure 5 The diagram of measuring the strength with Cu-9Ni-3Sn sample

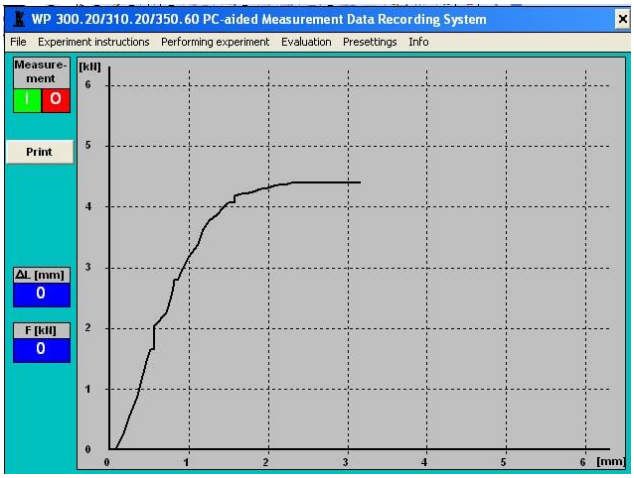

Figure 6 The diagram of measuring the strength with Cu-9Ni-6Sn sample

Figure 5 and Figure 6 show that the mechanical properties changed more as assembling the quenching, strain and tempering within two hours. The measurement results of the mechanical properties show that: The S_1 sample with 0.98mm of thickness, 10mm^2 of cross-section area, 1060MPa of tensile strength, and 903MPa of elastic limit, after tempering, the average hardness is 240HV. The S_2 sample with 0.98mm, 10mm^2 of cross-section area, 1282MPa of tensile strength, and 1137MPa of elastic limit, after tempering, the average hardness is 282HV.

The increasing hardness gives an expression that, in the samples, a phase transformation occurs. The product of this transformation cannot be seen. However, when it is observed by using the optical microscopy, it may be extremely small in size of a new phase, and equivalent to the Spinodal cluster. With the small size in a uniform distribution, these clusters increase their strength strongly. Nonetheless, more modern-equipments must be used to confirm and observe this Spinodal cluster. The similar results related to mechanical properties of Cu-Ni-Sn alloys are reported in the published studies [6, 19, 23].

3.2 Roughen diffraction (X-ray)

X-ray diffraction analysis of Cu-9Ni-3Sn after aging at 350^{o}C shown in Figure 7. It can be seen that this is a single phase structure. Meaning, the lattice is still a solid-solution one, which further confirms that, at this aging temperature, the solution lattice is constant, many small areas of different components causing the dislocation of the lattice result in increasing the strength and the hardness.

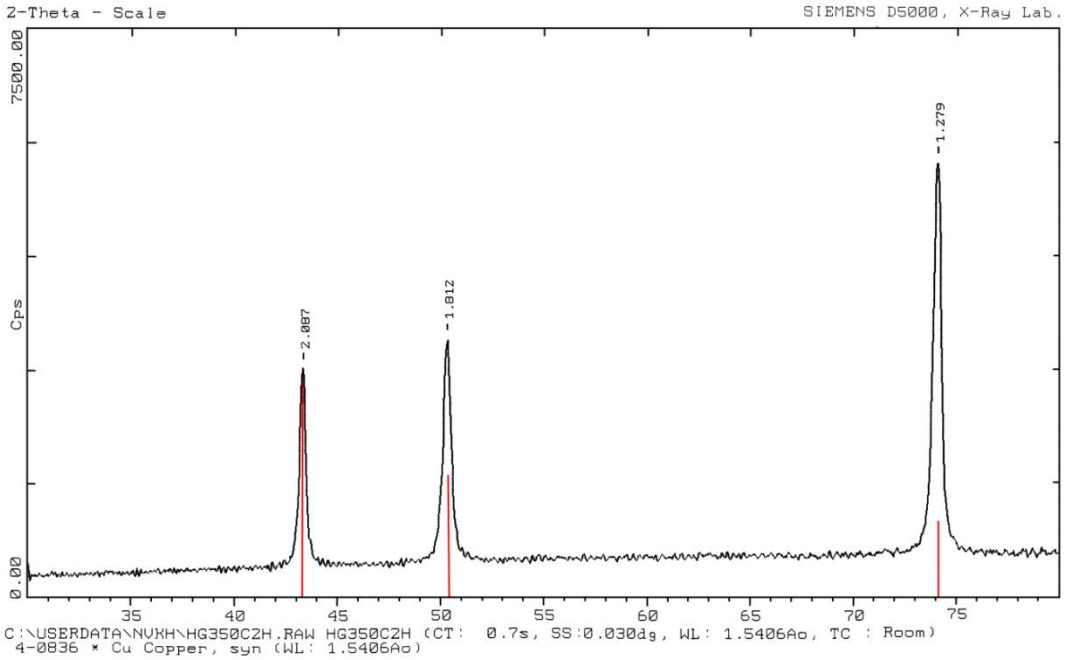

Figure 7 X-ray diffraction of Cu-9Ni-3Sn after aging at 350°C

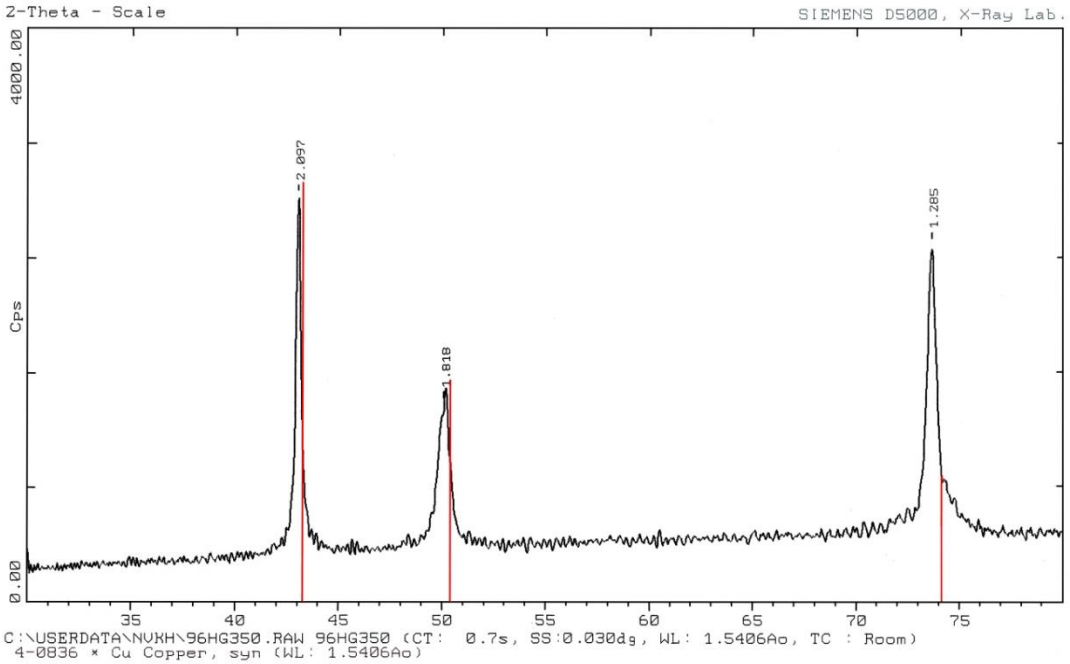

Figure 8 X-ray diffraction of Cu - 9Ni – 6Sn after aging at 350°C

From Figure 7, it can be seen that the lattice size (d) increases in comparison with the standard size of the copper, the diffraction peaks did not follow the rules of the coppery diffraction diagram, namely the peak at the 3rd position (311) is higher than the peak at the 1st position, and the peaks tend to deviate to the left of the graph. This can be proved that Sn has "crept into" and replaced some peaks of the Cu-Ni solution-solid causing the dislocation of the lattice structure, thus the durability of the material increases. Based on the image about microstructure, FESEM, and diffraction diagram, any second phase cannot be find. Hence, it can be assumed that there is a new type of structure that is supposed to be the Spinodal cluster distribution. In addition, the peak at the 3rd position is significantly higher than the 1st position. This may be explained that the deformation has transformed the lattice structure and left the residual stresses of the deformation process.

Parameters: Cu electrode, radiation $K_{\alpha 1}$, wave

length λ = 1.05406A^0; d(111) = 2.087A^0; d(200) = 1.812A^0; d(220) = 1.279A^0. With the d-face distance values and the 2θ diffraction patterns on the gauge, the structures parameters for the FCC are determined as given in Table 5.

Table 5 Structure parameters of the Cu-9Ni-3Sn alloy after deformation and aging at 350^{0}C during 2h

No	(hkl)	Structure	Cu-9Ni-3Sn alloy after deformation, aging at 350^{0}C, 2h		
			d_{hkl}[A^0]	2θ(°)	a[A^0]
1	(111)	FCC	2.087	43.3570	3.6078
2	(200)	FCC	1.812	50.3598	3.6240
3	(220)	FCC	1.279	74.1365	3.6175

The diffraction lines in Figure 7 are corresponding to the lines of Cu with the faces (111), (200) and (220) for the FCC with 3.61A^0 of the structure constant of Cu. The lines show that it is a solid solution of Cu. The lines are almost identical to the Cu traces, although the trailing edge (200) deviated slightly from the baseline due to the alloying and structure deformation along with the presence of the Spinodal cluster. The structure parameters are equal to Cu's structure parameters.

From Figure 8, it can be seen that after performing the deformation process combined with aging and the common characteristics of being compared to the no-deformation process, the peak at the 3rd position has a higher energy than the 1st position. The difference can be understood that the prior orientation of the deformation process remains after deforming, and it is proved clearly on the SEM images.

Parameters: Cu electrode, radiation $K_{\alpha 1}$, wave length λ = 1.05406A^0; d(111) = 2.097A^0; d(200) = 1.818A^0; d(220) = 1.285A^0. With the d-face distance values and the 2θ diffraction patterns on the gauge, the structured parameters for the FCC are determined as given in Table 6.

Table 6 Structure parameters of the Cu-9Ni-3Sn alloy after deformation and aging at 350^{0}C during 2h

No	(hkl)	Structure	Cu-9Ni-3Sn alloy after deformation, aging at 350^{0}C, 2h		
			d_{hkl}[A^0]	2θ(°)	a[A^0]
1	(111)	FCC	2.097	43.1401	3.6321
2	(200)	FCC	1.818	50.1821	3.6360
3	(220)	FCC	1.285	73.7329	3.6345

The diffraction lines in Figure 8 are corresponding to the lines of Cu with the faces (111), (200) and (220) for the FCC. These lines moved to the left of the standard lines of Cu show that this is a solid solution of Cu with Ni and Sn. The distance of the three-faceted surface index is about 3.63A^0, which is higher than that of 3% Sn alloying.

3.3 SEM Analysis

By using scanning electron microscopy with S_1 (at 150.0k), the product of this transformation can be seen from Figure 9, where the size of the grain is very small (less than 50nm) and scattering on the sample's cross section. The increase in the value of the strength and hardness is explained by the deformation mechanism.

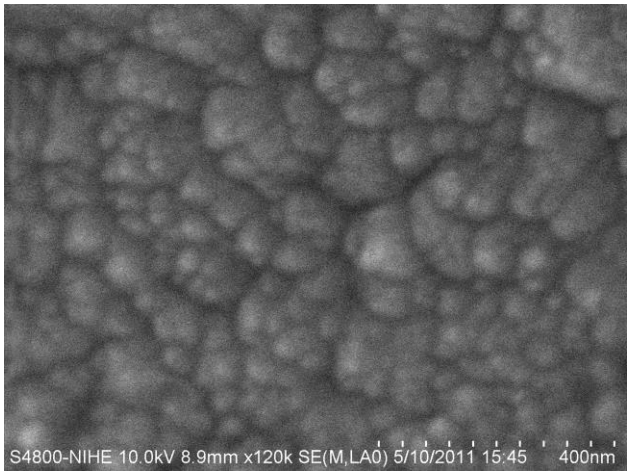

Figure 9 SEM of Cu-9Ni-3Sn

For S_2 sample, by using scanning electron microscopy (at 220.0k), the product of this transformation can be observed and shown in Figure 10. The size of the new phases is very small (less than 100nm), and the new phases are scattered on the sample's cross-section area. These new phases include Spinodal cluster to increase the strength for this alloy. This Spinodal cluster is the characteristic of Spinodal and deformation decomposition.

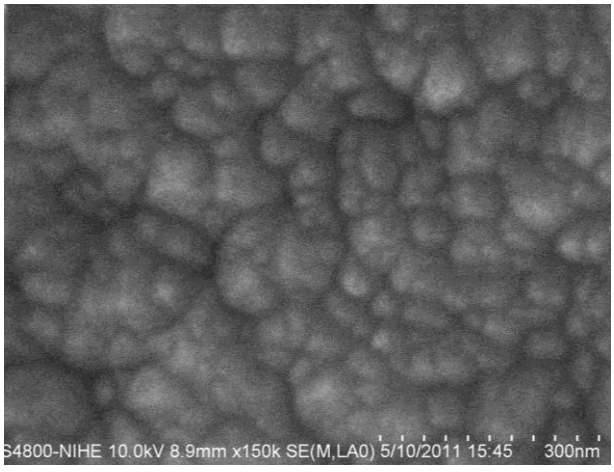

Figure 10 SEM of Cu-9Ni-6Sn

The analysis result of the sample after deforming and aging shows that the sizes of alloy structure are fine, and the deformation orientation still appears right after aging. Along with the aging, in the alloy structure, there is also a knotted structure that can be conjectured, it is a structural type of Spinodal distribution.

Based on the elemental distribution plot, the high mass of Sn element is concentrated on the particle boundaries compared to the distribution of elements inside the particle. This evidenced can be seen clearer by observing the distribution mapping of Cu, Ni, Sn elements inside the particle and at the particle boundary. The results are shown in Figure 11 and Figure 12.

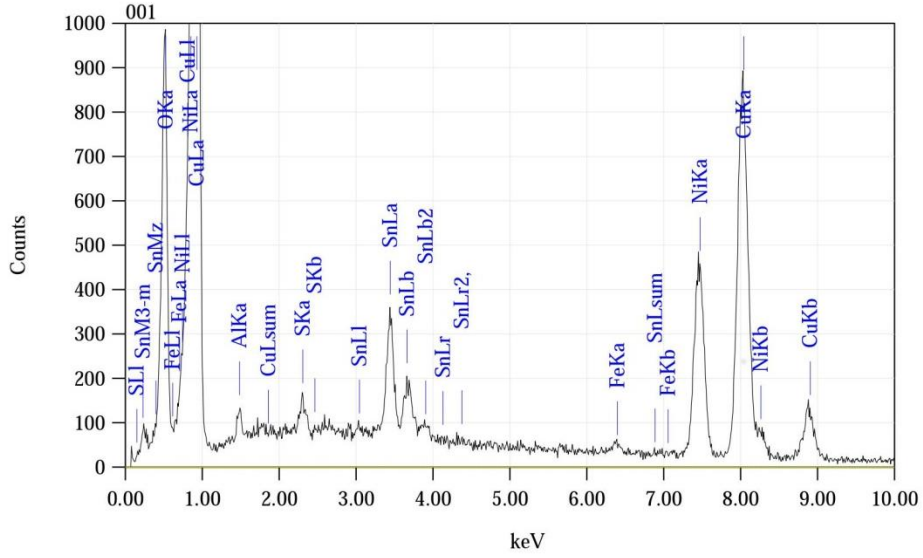


```
Acquisition Parameter
Instrument    : 6490(LA)
Acc. Voltage : 20.0 kV
Probe Current: 1.00000 nA
PHA mode      : T4
Real Time     : 64.94 sec
Live Time     : 50.00 sec
Dead Time     : 22 %
Counting Rate: 2426 cps
Energy Range :  0 - 20 keV
```

ZAF Method Standardless Quantitative Analysis
Fitting Coefficient: 0.2722

Element	(keV)	Mass%	Error%	Atom%	Compound	Mass%	Cation	K
O K	0.525	18.14	0.13	46.78				17.7575
Al K	1.486	1.03	0.16	1.57				0.4098
S K	2.307	0.75	0.08	0.96				0.6702
Fe K	6.398	0.62	0.22	0.46				0.7326
Ni K	7.471	20.87	0.38	14.67				22.1784
Cu K	8.040	50.29	0.50	32.67				50.9893
Sn L	3.442	8.30	0.27	2.88				7.2622
Total		100.00		100.00				

Figure 11 The elemental distribution plot for Cu-9Ni-3Sn sample

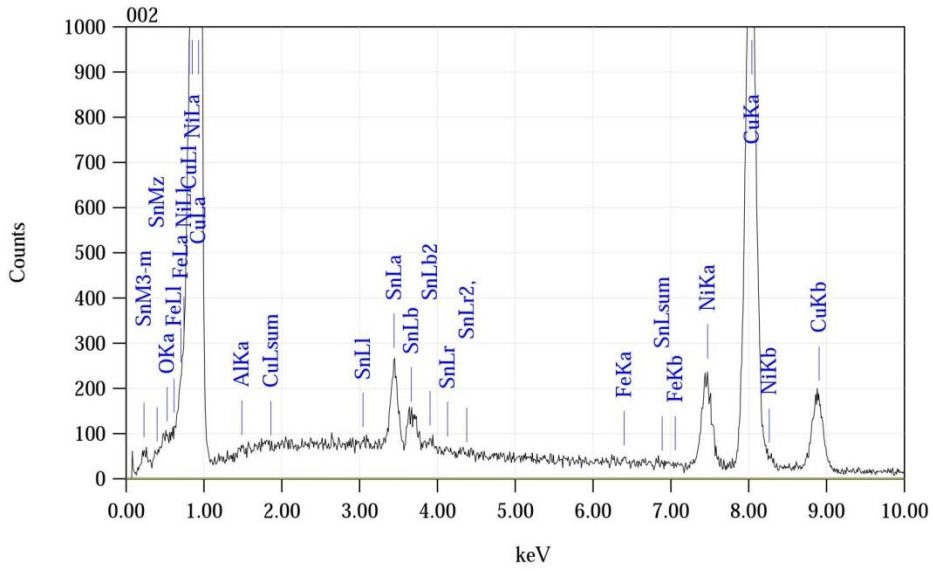


```
Acquisition Parameter
Instrument    : 6490(LA)
Acc. Voltage  : 20.0 kV
Probe Current: 1.00000 nA
PHA mode      : T4
Real Time     : 65.67 sec
Live Time     : 50.00 sec
Dead Time     : 23 %
Counting Rate: 2608 cps
Energy Range :  0 - 20 keV
```

```
ZAF Method Standardless Quantitative Analysis
Fitting Coefficient : 0.2652
Element          (keV)    Mass%   Error%    Atom%  Compound    Mass%  Cation          K
 O K             0.525     0.09     0.19     0.36                                  0.0847
Al K             1.486     0.23     0.24     0.55                                  0.0834
Fe K             6.398     0.22     0.30     0.26                                  0.2666
Ni K             7.471    10.36     0.53    11.39                                 10.9270
Cu K             8.040    82.61     0.70    83.91                                 83.1721
Sn L             3.442     6.48     0.40     3.53                                  5.4663
Total                    100.00           100.00
```

Figure 12 The elemental distribution plot for Cu-9Ni-6Sn sample

3.4 Electrical Conductivity

Electrical conductivity test result for S_1 sample with different heat treatments is shown in Table 7 and Table 8.

Table 7 The S_1 sample size for electrical conductivity test

No	Heat treatment	Length l, m	Width a, m ($x10^{-3}$)	Thickness b, m ($x10^{-3}$)	Cross-section area F, m^2 ($x10^{-6}$)
1	After cold-rolled 40%	0.517	1.9	0.3	0.57
2	After cold-rolled 40% and aged at 350°C,	0.517	1.9	0.3	0.57

Table 8 The test result of S_1 electrical conductivity

No	Resistance R, Ω	Conductivity ρ, Ω.m ($x10^{-6}$)	Simen, S ($x10^6$)	%IACS
1	0.117	0.129	7.752	13.33
2	0.111	0.1224	8.167	14.08

The test results show that, after deforming and aging, the obtained high value of the electrical conductivity for S_1 sample is 14% of IACS, which fully corresponds to the requirements of the alloys used for the electrical contact. Thus, with the uniform heat treatment mode, which was 750°C of steeling, 40% of cold deformation and 350°C of aging, the obtained durability, the electrical conductivity of the sample is the highest and it is in accordance with the working condition of the electrical contact on high elastic and electrical conductivity.

Electrical conductivity test result for S_2 sample with different heat treatments is shown in Table 9 and Table 10.

Table 9 The S_2 sample size for electrical conductivity test

No	Heat treatment	Length l, m	Width a, m ($x10^{-3}$)	Thickness b, m ($x10^{-3}$)	Cross-section area F, m^2 ($x10^{-6}$)
1	After cold-rolled 40%	0.4	1.9	0.8	1.52
2	After cold-rolled 40% and aged at 350°C,	0.4	1.9	0.8	1.52

Table 10 The test result of S_2 electrical conductivity

No	Resistance R, Ω	Conductivity ρ, Ω.m ($x10^{-6}$)	Simen, S ($x10^6$)	%IACS
1	0.075	0.285	3.508	6.05
2	0.054	0.2052	4.873	8.40

The analysis of the electrical conductivity test results shows that the electrical conductivity value of the deformed and aged S_2 sample is 8.4% IACS. As a result, the electrical conductivity of S_1 sample is higher than S_2 sample. This is because the grain size of S_1 sample is smaller than the S_2 sample. These results are similar with the published study [14, 24].

4.0 CONCLUSION

Some important properties of Cu-Ni-Sn alloys can be concluded that the tensile strength values of Cu-Ni-Sn alloys including Cu-9Ni-3Sn (3% mass of Sn) and Cu-9Ni-6Sn (6% mass of Sn) are very high after heat treatment. However, tensile strength and the elastic limit of the Cu-9Ni-6Sn alloy are higher than those of Cu-9Ni-3Sn alloy. The hardness of Cu-9Ni-3Sn alloy increases by 37.27%, and of the Cu-9Ni-6Sn alloy increases by 116.80% compared to the hardness of the same alloys before heat treatment. Regarding the electrical conductivity, Cu-9Ni-3Sn alloy shows the higher electrical conductivity in comparison with Cu-9Ni-6Sn alloy. In addition, the increase in hardness, tensile strength, and the elastic limit of the Cu-9Ni-3Sn alloy after strain and tempering may be due to the deformation and the production of small grain, while Spinodal decomposition mechanism may be used to explain the increase in the above-mentioned hardness values for the Cu-9Ni-6Sn alloy.

Acknowledgment

The authors acknowledge Ho Chi Minh city University of Transport, Viet Nam Maritime University, Le quy Don University, Industrial University of Ho Chi Minh for supporting this research.

References

[1] Brush Wellman. 2001. Strengthening Mechanisms. *Technical Tidbits*. 3: 1-2.
[2] Duong, P. X., Tuan, H. A., Nam, N. D., and Vang, V. L. 2017. Effect of Factors on the Hydrogen Composition in the Carburizing Process. *International Journal of Applied Engineering Research*. 12(19): 8238-8244.
[3] Sahu, P., Pradhan, S. K., and De, M. 2004. X-ray Diffraction Studies of the Decomposition and Microstructural Characterization of Cold-worked Powders of Cu–15Ni–Sn Alloys by Rietveld Analysis. *Journal of Alloys and Compounds*. 337(1-2): 103-116.
[4] Fehim, F. 2012. Improvements in Spinodal Alloys from Past to Present. *Materials & Design*. 42: 131-146.
[5] Ilangovan, S., and Sellamuthu, R. 2013. Effects of Tin on Hardness, Wear Rate and Coefficient of Friction of Cast Cu-Ni-Sn Alloys. *Journal of Engineering Science and Technology*. 8(1): 34-43.
[6] Joshua, C., Ravikumar, V., John J. S. J., and John, J. L. 2008. Microstructural Effects on Tension and Fatigue Behavior of Cu–15Ni–8Sn Sheet. *Materials Science and Engineering: A*. 491(1-2): 137-146.
[7] Baburaj, E. G., Kulkarni, U. D., Menon, E. S. K.., and Krishnan, R. 1979. Initial Stages of Decomposition in Cu-9Ni-6Sn. *Journal of Applied Crystallography*. 12(5): 476-480.
[8] Nogita, K. 2010. Stabilisation of Cu_6Sn_5 by Ni in Sn-0.7Cu-0.05Ni Lead-free Solder Alloys. *Intermetallics*. 18(1): 145-149.
[9] Gupta, K. P. 2000. An Expanded Cu-Ni-Sn System (Copper-Nickel-Tin). *Journal of Phase Equilibria*. 21: 479.
[10] LourençoH, N., and Santos, H. 2005. Using Differential Scanning Calorimetry to Characterize the Precipitation Hardening Phenomena in a Cu-9Ni-6Sn Alloy. *Journal of Materials Engineering and Performance*. 14(4): 480-486.
[11] ASM Metal Handbook, Metallography and Microstructures. 2004.
[12] Copper Base Spinodal Alloy Strip and Process for its Preparation, US 4373970 A. http://www.google.ch/patents/US4373970, accessed on 2017-09-07.
[13] Highconductivity Coppers for Electrical Engineering, CDA Publication 122. 1998.
[14] Suzuki, S., Shibutani, N., Mimura, K., Isshiki, M., and Waseda, Y. 2006. Improvement in Strength and Electrical Conductivity of Cu-Ni-Si Alloys by Aging and Cold Rolling. *Journal of Alloys and Compounds*. 417(1-2): 116-120.
[15] Zhang, S., Jiang, B., Ding, W. 2010. Dry Sliding Wear of Cu-15Ni-8Sn Alloy. *Tribology International.* 43(1-2): 64-68.
[16] Zhang, S. Z., Jiang, B. H., and Ding, W. J. 2008. Wear of Cu-15Ni-8Sn Spinodal Alloy. *Wear*. 264(3-4): 199-203.
[17] Nagayoshi, H., Nishijima, F., and Watanabe, C. 2006. Bend Formability and Microstructure in a Cu-4 mass%Ni-1mass %Si-0.02 mass% P Alloy. *Journal of the Japan Institute of Metals and Materials*. 70(9): 750-755.
[18] Marcella, G. C. X., Clarissa, B. C., Rafael, K., Bismarck, L. S., Amauri, G., Noé, C., and José E. S. 2017. Directional Solidification of a Sn-0.2Ni Solder Alloy in Water-cooled Copper and Steel Molds: Related Effects on the Matrix Micromorphology, Nature of Intermetallics and Tensile Properties. *Journal of Alloys and Compounds*. 723(5): 1039-1052.
[19] Monzen, R., and Watanabe, C. 2008. Microstructure and Mechanical Properties of Cu-Ni-Si Alloys. *Materials Science and Engineering:* A. 483–484:15, 117-119.
[20] Chieu, L. T., Thang, S. M., Nam, N. D., and Khanh, P. M. 2016. The Effect of Deformation on Microstructure of Cu-Ni-Sn Aging Alloys, Engineering and Technology on Non-Ferrous Metals. *Key Engineering Materials*. 682: 113-118.
[21] Favass, E. P., and Mitropoulos, A. C. 2008. What is Spinodal Decomposition. *Jounal of Engineering Science Anh Technology Review*. 25-27.
[22] Zhao, C., and Notis, M.R. 1998. Spinodal Decomposition, Ordering Transformation, and Discontinuous Precipitation in a Cu-15Ni-8Sn alloy. *Acta Metallurgica*. 46(12): 4203-4218.
[23] Alili, B., Bradai, D., and Zieba, P. 2008. On the Discontinuous Precipitation Reaction and Solute Redistribution in a Cu-15% Ni-8% Sn Alloy. *Materials Characterization*. 59(10): 1526-1530.
[24] Vuorinen, V., Laurila, T., Mattila, T., Heikinheimo, E., and Kivilahti, J. K. 2007. Solid-State Reactions between Cu(Ni) Alloys and Sn. *Journal of Electronic Materials*. 36(10): 1355-1362.